Theoret. chim. Acta (Berl.) 22, 111—129 (1971)

Commentationes

Non-Empirical Interpretation of Nitrogen 14 Nuclear Quadrupole Coupling Constants

E. KOCHANSKI and J. M. LEHN
Institut de Chimie, 1 rue Blaise Pascal, 67-Strasbourg, France

B. LEVY
Laboratoire de Chimie de l'E.N.S., 24 rue Lhomond, 75-Paris 5ème, France

Received December 22, 1970

The ^{14}N nuclear quadrupolar coupling constants have been calculated for a series of nitrogen containing molecules from *ab initio* SCF–LCAO–MO wavefunctions built on basis sets of Gaussian type atomic functions. The various nuclear and electronic (from MO's, atoms, basis functions) contributions to the total field gradient have been analyzed and their relation to molecular and electronic structure is discussed.

The effect of the nature of the basis set on the accuracy of the computed field gradients has also been studied.

Les constantes de couplage quadrupolaire nucléaire de ^{14}N ont été calculées pour une série de composés azotés à partir de fonctions d'onde *ab initio* SCF–LCAO–MO (Hartree-Fock) construites sur une base de fonctions atomiques gaussiennes. Les diverses contributions nucléaires et électroniques (provenant des orbitales moléculaires, des atomes, des fonctions atomique de base) au gradient de champ total ont été analysées et reliées aux caractéristiques structurales des molécules considérées.

L'effet de la nature de la base de fonctions atomiques sur la précision des gradients de champs calculés a aussi été étudié.

Die ^{14}N-Kernquadrupol-Kopplungskonstanten sind für eine Reihe von N-haltigen Verbindungen aus *ab initio*-Wellenfunktionen, die auf Gauß-Orbitalen basieren, berechnet worden. Die einzelnen Kern- und Elektronenbeiträge zum Feldgradienten wurden untersucht und diskutiert, desgleichen der Einfluß des Typus der Basis auf die Genauigkeit der Resultate.

1. Introduction

The interaction of the nuclear quadrupole moment eQ (nuclei with spin $\geqq 1$) with the electric field gradient eq (arising from the nuclear and electronic charge distributions) at the site of the nucleus, represented by the nuclear quadrupole coupling constant $\chi_{ii} = e^2 q_{ii} Q/h$, gives rise to a manifold of physical effects of theoretical and practical significance [1–3]. Nuclear quadrupole interactions have been subject of numerous investigations in spectroscopy (microwave, magnetic resonance), solid state physics, molecular dynamics (through nuclear quadrupole relaxation), theoretical chemistry, etc. Because of this very broad

impact in physics and chemistry it is of prime importance to be able to interpret the quadrupolar coupling constants in terms of molecular structure and to calculate the components of the field gradient tensor eq from molecular wave functions.

Several semi-empirical methods have been used for calculating χ values and relating them to structural features and to electronic distributions [1–7]. Recently all electron Hartree-Fock-SCF–LCAO–MO wave-functions have become available for molecules of moderate size. The computation of eq then serves several purposes: testing the quality of the wave-functions, predicting quadrupole coupling effects in spectroscopy etc., providing a complete non-empirical basis for the interpretation of quadrupolar coupling constants in terms of molecular structural (and eventually conformational) features.

Among the quadrupolar nuclei, the ^{14}N nucleus is of special importance since it is widely distributed in a great variety of systems in organic, inorganic and biological chemistry.

We present here a detailed study of the origin of field gradients at nitrogen 14 nuclear sites in a number of cyclic and acyclic molecules [8].

Non-empirical studies of ^{14}N nuclear quadrupole coupling in some other systems (especially cyano, X–CN, compounds) have also appeared recently [9–15].

2. Results

2.1. Method of Calculation

The field gradient tensor eq_I is given by [9]:

$$eq_I = e\left[\sum_{K \neq I} \frac{Z_K(3R_{IK}R_{IK} - R_{IK}^2 1)}{R_{IK}^5} - 2\sum_{i=1}^{n}\sum_{k,l=1}^{M} c_{ki}c_{li}\left\langle \varphi_k \left| \frac{3r_I r_I - r_I^2 1}{r_I^5} \right| \varphi_l \right\rangle\right] \tag{1}$$

with:

eq_I: field gradient tensor at the quadrupolar nucleus I
Z_K: charge of nucleus K
R_{IK}: vector from nucleus I to K
1: unit dyadic
r_I: nucleus I to electron vector
n: number of doubly occupied MO's Φ_r

building up the single-determinental wavefunction Ψ

$$\Psi = [(2n!)]^{-1/2}|\Phi_1\alpha(1)\Phi_1\beta(2)\ldots\Phi_n\beta(2n)|\,. \tag{2}$$

M, φ_k, c_{ki}: number M of atomic orbitals φ_k in the basis set of the Φ_r expansions:

$$\Phi_r = \sum_{k=1}^{M} c_{kr}\varphi_k \tag{3}$$

where the c_{kr} are known expansion coefficients.

A programme has been written [16], which calculates the diagonal and off-diagonal elements of the nuclear and electronic contributions to the field gradient tensor in an arbitrary coordinate axis system x, y, z.

The method of calculation of the one-, two- and three-center integrals over atomic orbitals φ_k in Eq. (1) is described elsewhere [16]. The atomic orbitals are gaussian type functions (GTF).

The wavefunctions used are of the SCF–LCAO–MO type and have been obtained in this or in other laboratories. They were all built on a basis set of GTF's grouped into sets of contracted GTF's (CGTF's) and have been obtained with the general programme IBMOL [17]. In some cases wavefunctions of different qualities have been used for the same molecule.

After calculating eq, the programme diagonalizes the field gradient tensor and computes the orientation of the principal axis system (X, Y, Z) of the field gradient tensor with respect to the initial x, y, z coordinate axes, and the components of eq in the X, Y, Z axis system. Multiplying by eQ_N gives then the X, Y, Z components of the nitrogen quadrupolar coupling constant. The output of the programme consists of the components of the total field gradient and of its decomposition into various contributions (see below 2.2).

2.2. Comments on Calculations and Results

The electric field gradient at the nitrogen site(s) has been calculated in the following molecules:

pyrrole I, pyrazole II, imidazole III, isoxazole IV, oxazole V, pyridine VI, pyrazine VII, diazirine VIII, diimide IX, ammonia X, ethylene imine XI, methylene imine XII, carbodiimide XIII, hydrazine XIV and borazane XV. For X, XI and XII both the most stable form and the transition state for nitrogen inversion have been studied.

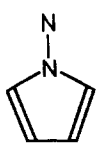

I

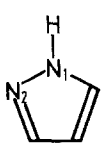

II

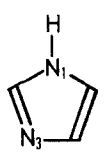

III

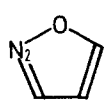

IV

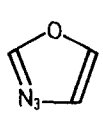

V

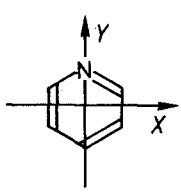

VI

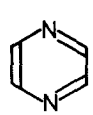

VII

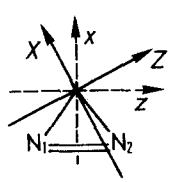

VIII

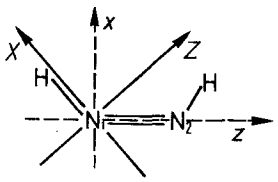

IX *(cis)*
(<zN₁H=63°)

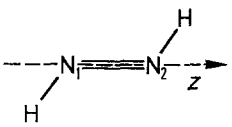

IX *(trans)*
(<zN₁H=70)

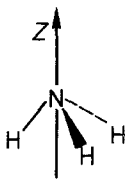

X

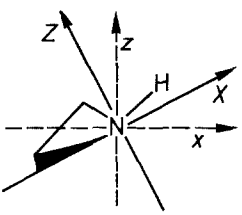

XI *(pyramidal)*

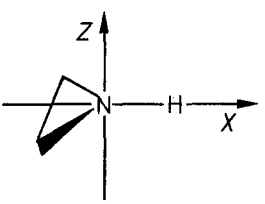

XI *(planar)*

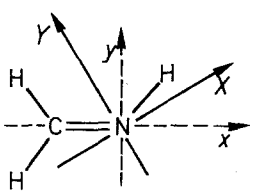

XII *(bent)*
(<xNH=67°)

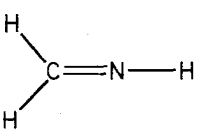

XII *(linear)*

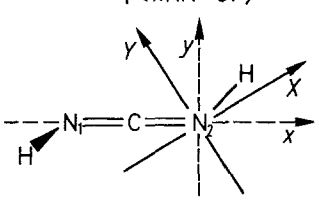

XIII
(<xNH=60°)

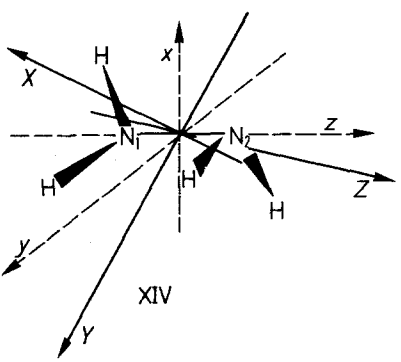

XIV

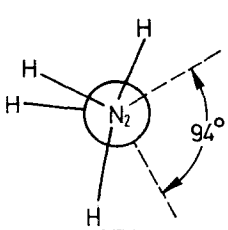

XIV
(Newman projection)

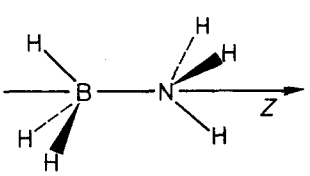

XV

The wavefunctions have been obtained from the following references: I [18], II–V [19], VI [20], VII [21], VIII [22], IX [23], X [24], XI [25], XII [23, 26], XIII [23], XIV [27], XV [28]. These wavefunctions are composed of delocalized MO's except for compounds II–V, where localized MO's were available [19]. They are of varied accuracy, depending of the size of the basis set of GTF's and on the type of contraction used for building up the CGTF's. Table 1 lists the basis sets used. The fact that the *s* type GTF's have an improper shape near the origin should not affect much field gradient calculations even with relatively small basis sets, since the major electronic contribution arises mainly from the 2*p* functions of nitrogen, which behave correctly near the nucleus [11]. A sufficiently flexible basis set should automatically take care of the Sternheimer core polarisation [29], so that no special correction has been made although the smaller basis sets used for the present systems are less satisfactory than the larger ones.

In order to compute the quadrupolar coupling constant component ($e^2 q_{ii} Q/h$) to be compared with the experimental values it is necessary to know the ^{14}N nuclear quadrupole moment eQ. The only value of eQ based exclusively on experimental data (microwave data on the NO molecule) is quite inaccurate: $1.6 \pm 0.7 e \times 10^{-26}$ cm^2 [30]. Combining calculations of eq with accurate SCF wavefunctions and experimental e^2qQ/h data, the following values have been obtained: $1.47 e \times 10^{-26}$ cm^2 [9, 10], $1.56 e \times 10^{-26}$ cm^2 [12], $1.66 e \times 10^{-26}$ cm^2 [13]. In view of these results, we used a value of $1.6 e \times 10^{-26}$ cm^2 which is probably within 10% of the real value.

Table 1 lists the computed total $e^2 q_{ii} Q/h$ components (χ_{ii}) for the various substances I–XV and basis sets, the asymmetry parameters η (defined as $\eta = |\chi_{\alpha\alpha} - \chi_{\beta\beta}|/|\chi_{\gamma\gamma}|$ with $|\chi_{\alpha\alpha}| \leqq |\chi_{\beta\beta}| \leqq |\chi_{\gamma\gamma}|$), the orientation of the principal field gradient axis system X, Y, Z with respect to the coordinate axis system x, y, z and the corresponding available experimental data.

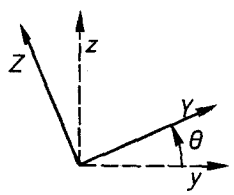

Microwave data are generally gas phase values for the inertial axis system unless off-diagonal components may be measured; in many cases the inertial and field gradient principal axis system coincide. Nuclear quadrupole resonance (NQR) leads to the solid state value of the largest $|\chi_{ii}|$ component in the X, Y, Z system and to $\eta \cdot |\chi_{ii}|$ values are expected to be smaller in the solid state than in the gas phase by about 0.3–0.5 MHz.

Tables 2–7 list analyses of the total field gradient into various contributions: analysis of the nuclear contribution into contributions from the different nuclei, analysis of the electronic contribution into contributions from the MO's, from the atoms and from the CGTF's.

Table 1. *Calculated and experimental*[a] ^{14}N *nuclear quadrupole coupling tensor components* χ_{ii}, *asymmetry parameter* η *and rotation angle* θ *for the principal axis system X Y Z (in MHz)*

Molecule		Basis set[b] Exp.(method)[a]	χ_{XX}	χ_{YY}	χ_{ZZ}	η	θ(axis)[c]	Ref.
I		B_1	−5.24	2.91	2.34	0.11	0°	
		exp.(MW)	−2.66	1.45	1.21	0.07	—	[31]
II	(at N(1))	B_1	−4.92	3.04	1.88	0.24	15°04′(x)	
		exp.(NQR)[d]	|2.6|	—	—	—	—	[32]
		exp.(MW)[e]	−3.018	1.641	1.377	—	—	[47]
II	(at N(2))	B_1	1.30	−6.32	5.01	0.59	−28°49′(x)	
		exp.(NQR)	—	|3.995|	—	0.657	—	[32]
		exp.(MW)[e]	0.794	−3.961	3.167	—	—	[47]
III	(at N(1))	B_1	−4.30	1.91	2.39	0.11	88°35′(x)	
		exp.(NQR)[d]	|1.7|	—	—	—	—	[32]
III	(at N(3))	B_1	1.45	−5.03	3.59	0.425	50°43′(x)	
		exp.(NQR)	—	|3.27|	—	0.129	—	[32]
IV		B_1	0.89	−6.01	5.12	0.70	−32°20′(x)	
		exp.(MW)[e]	<1	<1	<1	—	—	[33]
V		B_1	1.57	−4.98	3.41	0.31	51°10′(x)	
		exp.(MW)[e]	1.58	−3.99	2.41	0.21	—	[33]
VI		B_1	3.51	−6.30	2.79	0.115	0°	
		exp.(MW)	3.45	−4.88	1.43	0.405	—	[34]
VII		B_1	3.47	−6.62	3.15	0.05	0°	
		exp.(NQR)	—	|4.857|	—	0.536	—	[35]
VIII	(at N(1))[f]	B_2	−0.31(−0.68)	2.93(2.93)	−2.62(−2.25)	0.79(0.50)	23°28′(y)	
		B_3	−0.40(−0.86)	2.69(2.69)	−2.29(−1.8)	0.70(0.53)	29°40′(y)	[36]
		exp.(MW)[e]	$\lvert\chi_{AA}\rvert < 1$ MHz	$\chi_{cc} - \chi_{BB} = 6.2$ MHz		—	—	[37]
		exp.(MW)[g]	0.48	2.05	−2.53	0.62	—	[38]
		exp.(MW)[h]	−0.94	3.44	−2.23	0.37	0°	[39]
IX	*trans*(at N(1))	B_2	1.39	4.31	−5.70	0.51	59°16′(y)	
IX	*cis* (at N(1))	B_2	1.57	4.15	−5.72	0.45	63°(y)	
X	*(pyramidal)*	B_2	2.94	2.94	−5.87	0	0°	
		B_5	—	—	−3.94	0	0°	[14]
		exp.(MW)	—	—	−4.084	0	—	[40]
X	*(planar)*	B_2	3.50	3.50	−6.99	0	0°	
XI	*(pyramidal)*	B_1	4.36	1.48	−5.84	0.49	29°11′(y)	
		B_2	3.35	1.02	−4.37	0.52	25°54′(y)	
		B_3	3.00	0.57	−3.57	0.68	25°50′(y)	[36]
		exp.(MW)	3.004	0.685	−3.689	0.629	25°25′(y)	[41]
XI	*(planar)*	B_2	5.05	2.71	−7.76	0.30	0°	
XII	*(bent)*	B_1	3.21	−5.95	2.74	0.08	32°32′(z)	
		B_2	1.32	−4.97	3.65	0.47	34°40′(z)	
		B_2'	1.36	−4.52	3.16	0.40	33°18′(z)	
		B_4	1.24	−4.86	3.62	0.49	35°06′(z)	
		exp.(MW)[i]	1.9	−5.1	3.2	0.25	31°(z)	[42]
XII	*(linear)*	B_2	2.90	−8.02	5.11	0.28	0°	
XIII	(at N(2))	B_2	2.51	−2.55	0.04	0.97	~27°(z)[j]	
XIV	(at N(1))	B_6	−5.89	1.82	4.07	0.38	~42°(z)[j]	
		exp.(NQR)	|4.82|	—	—	0.80	—	[44]
XV	at N		1.13	1.13	−2.25	0	0°	
	at B[k]		−0.92	−0.92	1.84	0	0°	

3. Discussion

We shall analyse successively the origin and the structural effects on the electric field gradient at the ^{14}N nucleus in the different types of compounds, considering in turn the total field gradient and the various contributions.

Then, the effect of the basis set of atomic functions will be discussed and finally the various conclusions reached will be briefly summarized.

3.1. Five-Membered and Six-Membered Heterocycles I–VII

The wavefunctions used for the heterocyclic system I–VII were all built on the minimal basis set B_1 (see footnote b in Table 1). Systems I, VI and VII are described in terms of delocalized MO's, whereas localized MO's were available for the molecules II–V.

Total Field Gradient. Quadrupolar Coupling Constants (Table 1)

Inspection of the results listed in Table 1 leads to the following comments.

1) The agreement between calculated and experimental values of χ_{ii} is quite poor and is not better than in the case of semi-empirical calculations of the CNDO/2 type [45]. The discrepancy is especially large for the tricoordinated nitrogen sites in pyrrole I, pyrazole II (N(1)) and imidazole III (N(1)) where the

---

[a] Microwave (MW) and nuclear quadrupole resonance (NQR) are for gas and solid phase respectively. Coupling constants are probably 0.3–0.5 MHz larger in gas phase than in solid state.

[b] Basis sets of gaussian type functions (GTF) and contracted GTF's (CGTF):
B_1: (7.3/3; 2.1/1);
B_2: (9.5/4; 4.2(3.2/2), the two *p*CGTF's contain respectively 3 and 2 *p*GTF's;
B_2': (9.5/4; 4.2(4.1)/2), the two *p*CGTF's contain respectively 4 and 1 *p*GTF's;
B_3: (10.5/4; 4.2(4.1)/2);
B_4: (10.6/5; 5.3/3);
B_5: extended set of gaussian lobe functions;
B_6: (9.3/3) uncontracted.
Convention: (number of $s \cdot p$ (on heavy atom)/s (on H) GTF's; number of $s \cdot p$ (on heavy atom)/s (on H) CGTF's): ($s \cdot p/s$ GTF's; $s \cdot p/s$ CGTF's).

[c] Angle θ for transforming the coordinate axis system $x\ y\ z$ into the principal axis system $X\ Y\ Z$ of the field gradient by rotation about axis (i).

[d] Values obtained from the single NQR resonance reported in [32] assuming the same asymmetry parameter as in pyrrole.

[e] Values for the inertial axis system.

[f] Calculated values in parentheses are for the coordinate axis system $x\ y\ z$.

[g] MW data in inertial axis system for C-methyl diazirine. The inertial axis system is rotated by 28°24′ about the z axis with respect to the coordinate system $x\ y\ z$. These MW values cannot be compared directly to the calculated χ components.

[h] MW data for C-dimethyl diazirine in the inertial axis system which is identical with the coordinate system $x\ y\ z$ (χ values in parentheses).

[i] MW data for N-methyl methylene imine ($CH_2=N-CH_3$) in the inertial axis system. The orientation of this inertial axis system should be similar to that in propene ($CH_2=CH-CH_3$) which is rotated by 31° (z) with respect to the coordinate system $x\ y\ z$ [43].

[j] In these two cases rotations about more than one axis occur for the $(x, y, z) \rightarrow (X, Y, Z)$ conversion. Only the largest rotation is given; the other rotations are close to zero.

[k] A ^{11}B nuclear quadrupole moment eQ of $3.55e \times 10^{-26}$ cm^2 has been used.

Table 2. *Contributions to the* ^{14}N *electric field gradient (principal axis system)*[a]

	Pyrrole I								
	X	Y	Z	YZ		X	Y	Z	YZ
Nuclear contributions									
Total T_N	−0.94	0.36	0.58	0					
Electronic contributions									
MO					CGTF				
$6a_1(\sigma)$	−0.43	−0.41	0.84	0	xN(1), xN(1)	3.22	−1.61	−1.61	0
$4b_2(\sigma)$	−0.42	0.81	−0.39	0	yN(1), yN(1)	−0.86	1.72	−0.86	0
$8a_1(\sigma)$	−0.49	−0.45	0.94	0	zN(1), zN(1)	−0.97	−0.97	1.94	0
$1b_1(\pi, lp)$	1.51	−0.75	−0.75	0	zN(1), sH(1)	−0.11	−0.11	0.22	0
$2b_1(\pi, lp)$	1.75	−0.89	−0.87	0	Total T_E	0.46	−0.41	−0.04	0
Atoms									
N(1), N(1)	1.39	−0.86	−0.54	0					
C(2), C(2)	−0.20	0.18	0.02	0	Total $T_N - T_E$	−1.40	0.77	0.62	0
C(3), C(3)									
N(1), H(1)	−0.12	−0.12	0.25	0	χ_N	−5.24	2.91	2.34	0

[a] In this and in the following Tables only the largest contributions to *eq* are listed (generally $\geqq 0.15$). Because of the opposite charges of nuclei and electrons the total field gradient is $T_N - T_E$.

calculated values are about twice the experimental ones. However the values calculated for the dicoordinated =N– sites are in appreciably better agreement with the measurements, being about 50% larger. Considering the electronic contribution to the total field gradient (Tables 2–7), it is seen that in the case of dicoordinated N sites there are always two components $>|1|$, whereas for tricoordinated N sites all three components are weak ($<|0.3|$), because of partial canceling of individual contributions of opposite signs (see for instance the contributions of the MO's). Thus it is not surprising that less satisfactory computed values are obtained in the latter case.

2) The tricoordinated and dicoordinate nitrogen sites are easily distinguished, the former being characterized by lower values of the largest $|\chi_{ii}|$ component than the latter.

3) The principal axis system XYZ is oriented in such a way that the largest $|\chi_{ii}|$ component lies approximatily in the direction of the classical localized nitrogen "lone pair". For the tricoordinated nitrogen sites the largest component lies along the π type lone pair perpendicular to the molecular plane. For the dicoordinated =N– sites, the rotation angles $\theta = 51°10'$ and $50°43'$ calculated for the dicoordinated =N– sites in III (N(3)) and V are very near to the angle between the y axis and the bissector of the C(2)–N(3)–C(4) angle (*circa* 52°). In the case of II (N(2)) and IV, where one of the adjacent atoms is more electronegative than carbon, the principal axis system is rotated towards the more electronegative atom. Thus $\theta = 61°11'$ and $57°40'$ for N(2) in II and IV whereas the angle between the z axis and the X(1)–N(2)–C(3) bissector is about 70°. For all dicoordinated =N– sites the smallest χ component lies in the direction of the π system (χ_{XX}).

Table 3. *Contributions to the* ^{14}N *electric field gradient (principal axis system)* [a]

	Pyrazole, II at N(1)					at N(2)			
	X	*Y*	*Z*	*YZ*		*X*	*Y*	*Z*	*YZ*
Nuclear contributions									
Atom					Atom				
N(2)	−0.41	0.64	−0.23	0.44	N(1)	−0.41	−0.22	0.63	−0.45
C(4)	−0.08	−0.08	0.16	−0.01	C(3)	−0.36	0.12	0.24	0.54
C(5)	−0.35	0.04	0.32	−0.51	C(4)	−0.10	0.17	−0.08	0.04
H(1)	−0.15	−0.12	0.27	0.11					
Total T_N	−1.10	0.49	0.60	0.12	Total T_N	−0.99	0.19	0.80	0.02
Electronic contributions									
Localized MO					MO				
N(2) 1*s*	−0.12	0.18	−0.06	0.12	N(1) 1*s*	−0.12	−0.06	0.18	−0.13
N(1)–H	−0.82	−0.71	1.53	0.54	N(1)–N(2)	−0.65	−0.25	0.90	−0.80
N(1)–C(5)	−0.78	0.39	0.39	−1.19	N(2)–C(3)	−0.78	0.50	0.28	1.18
N(1)–N(2)	−0.74	1.23	−0.49	0.72	N(2) *lp*	−1.17	2.34	−1.16	−0.32
N(1) *lp*	3.15	−1.57	−1.58	−0.00	N(2)–C(3) π	1.49	−0.75	−0.74	0.06
					N(1) *lp*	0.17	−0.15	−0.02	−0.07
					C(4)–C(5) π	0.22	−0.09	−0.13	−0.01
Atoms					Atoms				
N(1), N(1)	1.27	−0.89	−0.38	0.06	N(1), N(1)	−0.31	−0.17	0.48	−0.35
N(2), N(1)	−0.12	0.23	−0.11	0.17	N(2), N(1)	−0.13	−0.10	0.22	−0.20
N(2), N(2)	−0.31	0.48	−0.17	0.30	N(2), N(2)	−0.43	1.83	−1.41	0.01
C(5), C(5)	−0.23	0.02	0.21	−0.33	C(3), C(3)	−0.23	0.08	0.15	0.35
H(6), N(1)	−0.13	−0.11	0.23	0.08					
CGTF					CGTF				
1*s*N(2), 1*s*N(2)	−0.13	0.20	−0.07	0.14	1*s*N(1), 1*s*N(1)	−0.13	−0.06	0.19	−0.14
*x*N(1), *x*N(1)	3.14	−1.57	−1.57	0	*x*N(2), *x*N(2)	1.85	−0.92	−0.92	0
*y*N(1), *y*N(1)	−0.85	1.70	−0.85	0	*y*N(2), *y*N(2)	−1.68	3.35	−1.68	0
*z*N(1), *s*H(1)	−0.11	−0.11	0.21	0.05	*z*N(2), *z*N(2)	−0.60	−0.60	1.19	0
*z*N(1), *z*N(1)	−1.02	−1.02	2.04	0					
Total T_E	0.21	−0.31	0.10	0.12	Total T_E	−1.34	1.87	−0.53	0.02
Total $T_N - T_E$	−1.31	0.81	0.50	0	Total $T_N - T_E$	0.35	−1.68	1.33	0
χ_N	−4.92	3.04	1.88	0	χ_N	1.30	−6.32	5.01	0

[a] See footnote to Table 2.

4) In the case of isoxazole IV and oxazole V the experimental χ_{ii} values are for the inertial axes whose orientation is unknown. For V the calculated and measured values are similar enough for suggesting that the inertial axes are near to the principal field gradient axes. This is not the case in isoxazole IV. It is found that the axis system, in which all three χ_{ii} components are smaller than |1|, corresponds to $\theta(x) \sim 15°$ ($\chi_{xx} = 0.89$; $\chi_{yy} = 0.01$; $\chi_{zz} = -0.90$). Thus an approximate orientation of the inertial principal axis system in IV is obtained.

Nuclear Contributions to the Field Gradient

The main nuclear contributions to the field gradient at the nitrogen sites in compounds I–VII, arise from the directly linked atoms (see Tables 2–7). Nuclei

Table 4. *Contributions to the* ^{14}N *electric field gradient (principal axis system)* [a]

	Imidazole, III at N(1)					at N(3)			
	X	Y	Z	YZ		X	Y	Z	YZ
Nuclear contributions									
Atom					Atom				
C(2)	−0.35	0.06	0.29	−0.52	N(1)	−0.09	0.15	−0.06	0.08
N(3)	−0.09	0.15	−0.06	−0.08	C(2)	−0.36	0.04	0.32	0.52
C(4)	−0.08	0.15	−0.06	0.07	C(4)	−0.35	0.09	0.25	−0.51
C(5)	−0.35	0.01	0.34	0.50					
H(1)	−0.15	0.31	−0.15	0.01					
Total T_N	−1.06	0.66	0.40	−0.01	Total T_N	−0.91	0.41	0.50	−0.03
Electronic contributions									
Localized MO					MO				
N(1)–H	−0.85	1.71	−0.86	0.08	N(3) *lp*	−1.07	2.15	−1.08	0.04
N(1)–C(2)	−0.79	−0.09	0.87	−1.11	C(2)–N(3) σ	−0.76	0.59	0.70	1.11
N(1)–C(5)	−0.79	−0.22	1.01	1.04	N(3)–C(4)	−0.76	0.12	0.65	−1.13
N(1) *lp*	3.08	−1.55	−1.53	−0.00	C(2)–N(3) π	1.78	−0.91	−0.88	−0.04
Atoms					Atoms				
N(1), N(1)	1.08	−0.37	−0.71	0.00	C(2), C(2)	−0.24	0.03	0.21	0.36
C(2), C(2)	−0.23	0.05	0.18	−0.34	N(3), N(3)	−0.46	1.47	−1.02	−0.00
N(1), C(5)	−0.11	−0.05	0.16	0.22	N(3), C(4)	−0.11	−0.19	0.11	−0.25
C(5), C(5)	−0.23	0.01	0.21	0.33	C(4), C(4)	−0.13	0.07	0.16	−0.35
N(1), H(1)	−0.13	0.26	−0.13	0.01					
CGTF					CGTF				
xN(1), xN(1)	3.05	−1.52	−1.52	0	xN(3), xN(3)	1.78	−0.89	−0.89	0
yN(1), yN(1)	−1.04	2.08	−1.04	0	yN(3), yN(3)	−1.53	3.06	−1.53	0
zN(1), zN(1)	−0.93	−0.93	1.85	0	zN(3), zN(3)	−0.70	−0.70	1.41	0
Total T_E	−0.08	0.15	−0.23	−0.01	Total T_E	−1.29	1.74	−0.45	0
Total T_N–T_E	−1.14	0.51	0.63	0	Total T_N–T_E	0.38	−1.34	0.95	0
χ_N	−4.30	1.91	2.39	0	χ_N	1.45	−5.03	3.59	0

[a] See footnote to Table 2.

removed by more than one bond contribute much less. As expected the effect is larger the higher the atomic number (H < C < N < O); because of the short N–H bond the effect of a proton is relatively large when directly linked but is otherwise very weak. The total nuclear contributions are very similar for similar nitrogen sites in the different systems.

Electronic Contributions to the Field Gradient.

Molecular Orbitals. The use of localized MO's for compounds II–V (Tables 3–5) allows studying the effect of the various chemical "bonds". The nitrogen lone pair gives always the largest contribution. The effect is appreciably larger for tri-coordinated nitrogen sites (N(1) in II and in III), where the lone pair is almost a pure N(2*p*) orbital, than for dicoordinated nitrogen sites (N(2) in II and IV; N(3) in III and V) where the lone pair is an sp^2 hybrid orbital. It is however interesting

Table 5. *Contributions to the* ^{14}N *electric field gradient (principal axis system)* [a]

	Isoxazole, IV					Oxazole, V			
	X	*Y*	*Z*	*YZ*		*X*	*Y*	*Z*	*YZ*
Nuclear contributions									
Atom					Atom				
O(1)	−0.52	−0.33	0.85	0.50	O(1)	−0.10	0.16	−0.07	0.09
C(3)	−0.36	0.19	0.17	−0.54	C(2)	−0.36	0.05	0.31	0.53
C(4)	−0.09	0.18	−0.09	−0.02	C(4)	−0.35	0.08	0.26	−0.51
Total T_N	−1.08	0.14	0.93	0.05	Total T_N	−0.91	0.42	0.50	0.04
Electronic contributions									
Localized MO					Localized MO				
1*s* O	−0.13	−0.08	0.21	0.13	1*s* C(2)	−0.12	0.16	0.10	0.17
O *lp*	−0.08	−0.06	0.15	0.04	1*s* C(4)	−0.12	0.28	0.09	−0.17
O–N	−0.63	−0.27	0.90	0.75	C(2)–Nσ	−0.76	0.76	0.69	1.12
N–C(3)σ	−0.78	0.62	0.16	−1.17	N–C(4)	−0.76	0.93	0.67	−1.13
N *lp*	−1.09	2.17	−1.07	0.36	N *lp*	−1.06	2.13	−1.07	0.02
O *lp*	0.14	−0.16	0.02	0.08	C(2)–Nπ	1.77	−0.90	−0.87	0.04
N–C(3)π	1.52	−0.76	−0.76	−0.06					
C(4)–C(5)π	0.20	−0.08	−0.12	0.01					
Atoms					Atoms				
O, O	−0.42	−0.28	0.70	0.40	C(2), C(2)	−0.24	0.04	0.20	0.36
O, N	−0.13	−0.10	0.24	0.20	N, N	−0.49	1.45	−0.96	−0.00
N, N	−0.32	1.74	−1.43	0.01	C(4), C(4)	−0.23	0.06	0.17	−0.34
C(3), C(3)	−0.23	0.13	0.11	−0.34					
CGTF					CGTF				
1*s*O, 1*s*O	−0.14	−0.09	0.23	0.14	*x*N, *x*N	1.74	−0.87	−0.87	0
2*s*O, 2*s*O	−0.11	−0.07	0.19	0.11	*y*N, *y*N	−1.52	3.04	−1.52	0
*x*N, *x*N	1.84	−0.92	−0.92	0	*z*N, *z*N	−0.71	−0.71	1.43	0
*y*N, *y*N	−1.61	3.21	−1.61	0					
*z*O, *z*O	−0.10	−0.04	0.15	0.12					
*z*N, *z*N	−0.55	−0.55	1.10	0					
Total T_E	−1.31	1.74	−0.43	0.05	Total T_E	−1.33	1.74	0.41	0.04
Total T_N–T_E	0.24	−1.60	1.36	0	Total T_N–T_E	0.42	−1.32	0.91	0
χ_N	0.89	−6.01	5.12	0	χ_N	1.57	−4.98	3.41	0

[a] See footnote to Table 2.

to note that the large contribution of the lone pair in the first case is almost entirely compensated by the contributions from the other MO's, whereas in the second case the contributions of the other MO's cancel out so that the total electronic contribution is almost equal to that of the lone pair.

The next important effects is due to the π bond directly attached to the nitrogen site (N(2) in II and IV; N(3) in III and V) and to the N–H bond (N(1) in II and III), followed by the directly linked σ bonds and then by the inner 1*s* shells of the neighbouring atoms.

Table 6. *Contributions to the* ^{14}N *electric field gradient (principal axis system)* [a]

	Pyridine, VI					Pyrazine, VII			
	X	Y	Z	XY		X	Y	Z	XY
Nuclear contributions									
Total T_N	0.84	0.08	−0.93	0	Total T_N	0.88	0.06	−0.94	0
Electronic contributions									
MO					MO				
$4b_2(\sigma)$	0.60	−0.29	−0.31	0	$4b_2(\sigma)$	0.58	−0.28	−0.31	0
$5b_2(\sigma)$	0.75	−0.36	−0.39	0	$5b_2(\sigma)$	0.74	−0.35	−0.39	0
$10a_1(\sigma)$	−0.20	0.45	−0.24	0	$1b_1(\pi)$	−0.24	−0.25	0.48	0
$1b_1(\pi)$	−0.29	−0.30	0.60	0	$10a_1(lp)$	−0.83	1.65	−0.83	0
$11a_1(lp)$	−1.32	2.65	−1.33	0	$2b_1(\pi)$	−0.58	−0.59	1.16	0
$2b_1(\pi)$	−0.54	−0.54	1.08	0	$11a_1(lp)$	−0.70	1.41	−0.71	0
Atoms					Atoms				
N(1), N(1)	−0.95	1.79	−0.84	0	N(1), N(1)	0.97	1.90	−0.93	0
N(1), C(2) N(1), C(6)	0.15	−0.06	−0.09	0.24	N(1), C(2) N(1), C(6)	0.16	−0.10	−0.07	−0.20
C(2), C(2) C(6), C(6)	0.28	−0.04	−0.23	−0.31	C(2), C(2) C(6), C(6)	0.30	−0.06	−0.25	−0.32
CGTF					CGTF				
$sC(2), sC(2)$ $sC(6), sC(6)$	0.15	−0.02	−0.13	0.17	$sC(2), sC(2)$ $sC(6), sC(6)$	0.16	−0.03	−0.13	0.17
xN, xN	1.49	−0.75	−0.75	0	$xN(1), xN(1)$	1.50	−0.75	−0.75	0
yN, yN	−1.66	3.32	−1.66	0	$yN(1), yN(1)$	−1.71	3.41	−1.71	0
zN, zN	−0.79	−0.79	1.57	0	$zN(1), zN(1)$	−0.77	−0.77	1.53	0
Total T_E	−0.09	1.76	−1.67	0	Total T_E	−0.04	1.82	−0.78	0
Total $T_N - T_E$	0.93	−1.67	0.74	0	Total $T_N - T_E$	0.92	−1.76	0.84	0
χ_N	3.51	−6.30	2.79	0	χ_N	3.47	−6.62	3.15	0

[a] See footnote to Table 2.

In the case of I, VI and VII, the results are less clear cut since the delocalized MO's have been used. However it is seen that again the lone pair and a π MO make up the largest contributions.

Considering the effect of *couples of atoms*, it is found that monocentric contributions are by far the most important ones, bicentric ones are weak and tricentric ones are even weaker. Similar nitrogen sites show similar monocentric contributions.

Turning now to the contributions of the various *atomic basis functions* (contracted gaussian type functions CGTF), it is seen that by far the most important effects arise from the $2p$ type functions on the nitrogen site considered, the largest effect being that of the $2p$ orbital making the smallest angle with the direction of the nitrogen lone pair ($2p_x$ for N(1) in I, II and III; $2p_y$ for N(2) in II and IV, N(3) in III and V, N(1) in VI and VII). The effects of the other CGTF's are all weak.

3.2. Azo Compounds VIII and IX

Table 1 shows that the calculated values of the χ components in diazirine VIII (coordinate axes x, y, z) are in reasonable agreement (within ca. 20%) with the experimental values obtained for 3,3-dimethyldiazirine by microwave spectroscopy (inertial axes identical with coordinate axes of VIII).

The largest $|\chi|$ component (χ_{ZZ}) is along the nitrogen lone pair in both forms of diimide but it is in the direction of the π bond (χ_{YY}) in diazirine; however in this latter case both lone pair and π components are of similar value. Comparing VIII to *cis* diimide, it is seen (Table 7) that, although the specific electronic effects introduced by the three membered ring play a role (especially for the X component of T_E), the main changes are of nuclear origin; these are particularly important for the χ_{ZZ} (lone pair) component which for VIII becomes smaller than χ_{YY} because $T_N(Z)$ compensates $T_E(Z)$ in a large part.

The largest nuclear contribution is that of the neighbouring nitrogen nucleus. The most important electronic contributions arise from the four highest lying MO's in both VIII and IX. These MO's describe the nitrogen lone pairs, the N–N, N–C, N–H σ bonds and the N–N π bond, and contain mainly (σ) or exclusively (π) N $2p$ atomic orbitals.

The monocentric electronic contribution is the most important, but a large bicentric effect arises also from the second nitrogen atom (Table 7).

Among the CGTF's, the most important contributions come from the $2p$ functions on nitrogen, especially from those which contain the GTF's with largest exponents (nearest to the nucleus).

3.3. Ammonia X and Aziridine XI

It is seen (Table 1) that the calculated χ components are in satisfactory agreement with experiment when wavefunctions built on extended basis sets are used (see below). The same holds for the orientation of the principal axis system of the field gradient in XI. The largest χ component (χ_{ZZ}) is lying along the direction of the nitrogen lone pair.

The largest nuclear contribution to the field gradient arises again from the atoms directly linked to the nitrogen site. Two MO's contribute very strongly to the field gradient in aziridine: 8*a* which is the highest occupied, nitrogen lone pair, MO and 4*b* which describes the (C–N) σ bonds using mainly $2p_y$ orbitals on the nitrogen site.

Again the CGTF's giving the strongest contribution are the N$2p$ functions containing the most compact GTF's. Similar results hold for ammonia.

The geometry of the nitrogen site is seen to have a strong effect on the quadrupolar coupling constant. When the nitrogen site becomes planar, i.e. in the transition state for nitrogen inversion, the components of the total field gradient increase markedly as both the nuclear and electronic terms increase. By far the largest individual increase is that of the contribution of the lone pair MO to the χ_{ZZ} component. Indeed when the nitrogen site becomes planar, the nitrogen lone pair becomes a pure $2p_z$ orbital, thus unbalancing even more the local electronic distribution.

Table 7. *Contributions to the* ^{14}N *electric field gradient (principal axis system)*[a]

Compound	Atomic, nuclear and total contributions					MO contributions				
	Atom	X	Y	Z		MO	X	Y	Z	
Diazirine, VIII, at N(1), (B_2)	N(1), N(1)	−0.04	−0.80	0.84	−0.11 (XZ)	$5a_1$(N–Nσ)	0.65	−0.62	−0.04	−0.74 (XZ)
	N(2), N(2)	−0.22	−0.43	0.65	0.47	$6a_1$(lp)	−0.41	−1.13	1.54	1.38
	C(3), C(3)	0.08	−0.19	0.11	−0.29	$2b_1$(π)	−0.69	1.32	−0.63	0.03
	T_N	−0.19	−0.85	1.03	0.17	$3b_2$(lp)	0.42	−0.68	0.26	−0.96
	$T_N - T_E$	−0.08	0.78	−0.70	0	T_E	−0.10	−1.63	1.73	0.17
Diimide, IX (*cis*) at N(1)	N(1), N(1)	−0.49	−1.09	1.58	−0.02 (XZ)	$3a_1$(N–Nσ)	1.61	−0.96	−0.65	0.76 (XZ)
	N(2), N(2)	0.59	−0.41	−0.18	−0.47	$4a_1$(lp)	−0.47	−1.10	1.57	−1.22
	N(1), H	0.14	−0.18	0.04	0.27					
	T_N	0.91	−0.72	−0.19	−0.50	$1b_1$(π)	−0.83	1.85	−0.97	−0.06
						$3b_2$(lp)	−0.66	−0.88	1.54	0.53
	$T_N - T_E$	0.42	1.10	−1.52	0	T_E	0.49	−1.82	1.33	−0.50
Diimide, IX (*trans*) at N(1)	T_N	0.84	−0.72	−0.12	0.52 (XZ)	T_E	0.47	−1.87	1.40	0.52 (XZ)
	$T_N - T_E$	0.37	1.44	−1.51	0					
Ammonia X (*pyramidal*), (B_2)	N, N	−0.86	−0.86	1.72	0 (XZ)	$1e_x$	2.53	−1.24	−1.28	
	N, H	0.30	−0.17	−0.13	−0.14	$1e_y$	−1.25	2.53	−1.28	
	T_N	0.16	0.16	−0.33		$3a_1$(lp)	−1.90	−1.90	3.80	
	$T_N - T_E$	0.78	0.78	−1.56		T_E	−0.62	−0.62	1.23	
Ammonia X (*planar*), (B_2)	N, N	−1.02	−1.02	2.04	0	$1e'_x$	2.52	−1.23	−1.29	
	N, H	0.33	−0.16	−0.16	0	$1e'_y$	−1.23	2.52	−1.29	
	T_N	0.21	0.21	−0.43		$1a''_2$(lp)	−2.06	−2.06	4.11	
	$T_N - T_E$	0.93	0.93	−1.86		T_E	−0.72	−0.72	1.43	
Ethyleneimine, XI (*pyramidal*), (B_2)	N, N	−0.84	−0.40	1.24	−0.09 (XZ)	4a''(C–Nσ)	−1.11	2.27	−1.16	−0.03 (XZ)
	C, C	0.16	−0.05	−0.11	−0.18	8a'(lp)	−0.95	−1.29	2.24	−1.09
	N, H	0.12	−0.18	0.06	0.28					
	T_N	0.56	−0.29	−0.27	−0.28	T_E	−0.33	−0.56	0.89	−0.28
	$T_N - T_E$	0.89	0.27	−1.16	0					
Ethyleneimine, XI (*planar*)	N, N	−1.26	−0.93	2.19	0 (XY)	4a''(C–Nσ)	−1.07	2.21	−1.11	0
	C, C	0.24	−0.05	−0.19	−0.25	8a'(lp)	−1.92	−1.92	3.83	0
	N, H	0.30	−0.15	−0.15	0					
	T_N	1.00	−0.29	−0.71	0	T_E	−0.34	−1.01	1.35	0
	$T_N - T_E$	1.34	0.72	−2.06	0					

Table 7 (continued)

Compound	Atomic, nuclear and total contributions					MO contributions				
	Atom	X	Y	Z		MO	X	Y	Z	
Methyleneimine, XII	N, N	−0.41	1.37	0.97	−0.02 (XY)	$5a'$(C–N σ)	1.16	−0.43	−0.73	0.61 (XY)
(bent), (B_2)	C, C	0.26	0	−0.26	−0.36	$1a''(\pi)$	−0.97	−1.01	1.98	−0.05
	N, H	0.20	−0.02	−0.19	0.26	$7a'(lp)$	−1.39	2.82	−1.44	−0.35
	T_N	0.61	−0.03	−0.59	−0.39	T_E	0.26	1.29	−1.56	−0.39
	$T_N - T_E$	0.25	−1.32	0.97	0					
Methyleneimine, XII	N, N	−0.77	2.23	−1.47	0	$5a_1$	1.82	−0.91	−0.91	0
(linear)	C, C	0.48	−0.24	−0.24	0	$1b_2(\pi)$	−0.89	−1.00	1.89	0
	N, H	0.29	−0.15	−0.15	0	$2b_1(lp)$	−1.80	3.60	−1.80	0
	T_N	1.15	−0.57	−0.59	0	T_E	0.38	1.57	−1.94	0
	$T_N - T_E$	0.77	−2.13	1.36	0					
Carbodiimide, XIII	N(2), N(2)	−0.76	0.73	0.03	0.03 (XY)	$6a$(CNH)	1.07	−0.51	−0.56	−0.01 (XY)
(at N(2))	C, C	0.40	−0.11	−0.29	−0.36	$7a$(CNH)	1.37	−0.68	−0.68	−0.004
	N(2), H(2)	0.18	−0.01	−0.16	0.23	$10a(lp)$	−0.85	0.14	0.71	−1.27
	T_N	0.88	−0.22	−0.66	−0.42	$11a(lp)$	−0.89	0.60	0.29	1.36
	$T_N - T_E$	0.67	−0.68	0.01	0	T_E	0.21	0.46	−0.67	−0.42
Hydrazine, XIV	N(1), N(1)	1.72	−0.57	1.14	0.01 (XZ)	$4a$(N–N)	−0.82	−0.47	1.29	0.84 (YZ)
(at N(1))	N(2), N(2)	−0.23	−0.27	0.50	0.20 (XZ)	$4b(lp)$	1.37	−0.63	−0.75	0.67 (XY)
	N(1), H(1)	−0.09	0.17	−0.08	0.16 (XY)					−0.23 (XZ)
					0.17 (YZ)	$5a(lp)$	1.59	−0.81	−0.78	−0.55 (XY)
	T_N	−0.46	−0.11	0.57	0.11 (XZ)					0.48 (XZ)
	$T_N - T_E$	−1.56	0.48	1.08	0	T_E	1.10	−0.60	−0.50	0.11 (XZ)
Borazane, XV	N, N	−0.37	−0.37	0.73	0	$4a_1$(B–N_z)	−0.93	−0.93	1.85	0 (XZ)
at N	B, B	−0.12	−0.12	0.22	0	$5a_1$(N–N_z)	−0.76	−0.76	1.52	0
						$1e$(N_x – H)	2.76	−1.37	−1.39	−0.03
	T_N	−0.08	−0.08	0.15	0	$2e$(N_y–H)	−1.37	2.76	−1.39	0.03
	$T_N - T_E$	0.30	0.30	−0.60	0	T_E	−0.38	−0.38	0.75	0
at B	B, B	0.12	0.12	−0.24	0	$5a_1$(B_z–N)	−0.17	−0.17	0.35	0
	N, N	−0.28	−0.28	0.55	0	$1e$(B_x–H)	0.65	−0.31	−0.34	0
	T_N	−0.22	−0.22	0.44	0	$2e$(B_y–H)	−0.31	0.65	−0.34	0
	$T_N - T_E$	−0.11	−0.11	0.22	0	T_E	−0.11	−0.11	0.22	0

[a] For the molecules listed in this Table, for which delocalized MO's were available, only the most important contributions to the electric field gradient are listed. More details may be obtained from the authors.

3.4. Methyleneimine XII and Carbodiimide XIII

In methyleneimine XII *(bent)* the largest χ component is again lying along the nitrogen lone pair, the second largest one being also in the plane of the σ system.

These two components are very similar to the corresponding in-plane components of χ found for the analogous nitrogen sites in III and in V. In carbodiimide XIII there are two components of almost equal value one along the lone pair direction and the other one also in the plane of the local σ system. Thus in comparison to methyleneimine, the analogous nitrogen site in carbodiimide displays a large decrease of the lone pair component. This is in good agreement with the dilution of the N(2) nitrogen lone pair into the adjacent N(1)=C double bond by conjugation, as already noted from the population analysis [23]. As a further indication, it is seen (Table 7), that whereas the nuclear contributions are not very different in XII and in XIII (difference <0.3), two of the electronic contributions are much weaker in XIII than in XII (difference of ca. 0.8).

The largest MO contributions in XII arise in decreasing order from the following MO's: the highest occupied, lone pair, MO $7a'$; the π bond MO $1a''$; the $5a'$ MO which describes in part the C–N σ bond and contains an important part of N($2p_y$) character.

When comparing these MO contributions to those found in carbodiimide XIII it is seen that in the latter case the main contributions arise from the low lying $6a$ and $7a$ MO's containing mainly $2p_x$ and $2p_y$ nitrogen atomic orbitals, followed by the two highest occupied, lone pair type, MO's $10a$ and $11a$ containing mainly N$2p_y$ and N$2p_z$.

In the transition state for nitrogen inversion in methylenimine, XII *(linear)*, a large increase of the quadrupolar coupling constants is observed, as in the XI *(planar)* form of aziridine. Again by far the largest change with respect to XII *(bent)* is found in the lone pair MO which becomes a pure $2p_y$ orbital in the XII *(linear)* form.

3.5. Hydrazine XIV and Borazane XV

The orientation of the principal field gradient axis system in hydrazine XIV is not as simple as in the other cases (see Fig. and Table 1). The largest χ component is distorted out of the intuitive lone pair direction, probably by the effect of N–N bond. The largest MO contributions arise from the MO's describing the nitrogen lone pairs and the N–N bond.

In borazane XV, the largest χ component lies along the B–N bond. It is however much weaker than in NH_3X *(pyramidal)*, as complexation of the nitrogen lone pair greatly reduces its contribution to the field gradient by diminishing the p electron unbalance (hydrogen bonding leads to similar effects [14]). The nuclear contributions are weak; the largest MO contributions arise from the MO's containing N$2p$ functions and describing the B–N and N–H bonds. The ^{11}B quadrupolar coupling constants calculated for H_3B–NH_3 are much lower than those measured for trialkylboranes (ca. |5| MHz [46]). This arises from the fact that the creation of the B–N bond removes the p electron defect present in boranes and partially balances out the B–H bonds. The ^{14}N and ^{11}B coupling constants are calculated to be very nearly the same in the eclipsed form of borazane as in its staggered conformation XV.

It is also interesting to note that the atomic contribution of B at N is much smaller than that of N at B (Table 7), which is similar to the effect of N(2) at N(1) in hydrazine. The monocentric term at B is smaller than the bicentric one due to N.

Including the effects of neighbouring O, C and H atoms a general trend is found: the *effect of directly linked atoms* on the field gradient at nitrogen decreases in the order O > N > C > B > H (see Tables 2–7). The effect of the vicinal N atom is also found to be larger in azo compounds (Sect. 3.2) than in hydrazine probably because of the shorter N, N distance in the former compounds.

3.6. Basis Set Effect on Calculated Field Gradients[1]

Basis set effects will be discussed principally on aziridine XI *(pyramidal)* and on methylenimine XII *(bent)* for which several different basis sets have been used.

The results listed in Table 1 show that the main basis set effect is found on changing from the minimal (7.3/3; 2.1/1) B_1 set to an extended set B_2, B'_2, B_3 or B_4 (see footnote b of Table 1).

1) The B_1 set leads to χ_{ii} values which are much higher (50% or more) than those obtained with an extended set. In CH_2NH the π component χ_{ZZ} and the χ_{XX} component are strongly altered in the B_1 case. Such large effects may explain the disagreement between the experimental and calculated χ_{ii} values (especially for the tricoordinated nitrogen sites) in the heterocycles I–VII for which basis set B_1 has been used.

2) The largest basis set effects are found when the nuclear and electronic contributions to a given χ_{ii} component are of opposite sign and of similar magnitude. This is the case for χ_{YY} in XI and for χ_{XX} in XII. Similar compensation effects among the various electronic contributions may also explain the worse results obtained for tricoordinated nitrogen sites as compared to dicoordinated ones in the nitrogen heterocycles I–III.

3) Inspection of the individual electronic contributions shows that the large variations due to the basis set occur for the terms (MO's, CGTF's) containing or representing p orbitals on the nitrogen site. It is worth noting that the change in contraction pattern of the p GTF's in basis sets B_2, B'_2 and B_3 brings about a relatively important change in χ_{ii} values (see VIII, XI, XII).

4) The orientation of the field gradient principal axis system, given by the rotation angle θ, is less sensitive to the basis set than the χ_{ii} components. It thus appears that minimal basis set (B_1) calculations may be used for predicting the direction of the field gradient axes within 5°.

4. Conclusion

The conclusions reached in the present work are of three types:

1) *Structural effects* on electric field gradients and quadrupolar coupling constants at nitrogen:

The principal component of the field gradient lies along the direction of the nitrogen lone pair (except in special cases like diazirine) for both tricoordinated

[1] For the definition of the various basis sets see footnote b of Table 1.

and dicoordinated nitrogen sites. Any structural effect leading to partial or complete disappearance of the lone pair decreases the field gradient: conjugation (in carbodiimide, in pyrrole or in other heterocycles as compared to methylenimine or ammonia), protonation (H^+, NH_3 system [14]), complexation (H_3B–NH_3).

Tricoordinated and dicoordinated nitrogen sites show characteristic field gradient components.

Adjacent N, O atoms lead to larger coupling constants. This may also hold for other heteroatoms (see also Sect. 3.5).

The nitrogen nuclear quadrupole coupling constants are very sensitive to the geometry at the nitrogen sites. Distortion towards the transition states of pyramidal or planar nitrogen inversion strongly increases the coupling constants.

The calculations give useful indications about the orientation of the inertial axis system as well as of the field gradient principal axis system.

2) *Nuclear and electronic contributions* to the field gradient:

By far the most important nuclear contributions arise from the adjacent atoms.

The largest MO contribution arises from the lone pair MO; followed by the π MO (in the case of dicoordinate nitrogen sites) and then by the X–N σ bond MO's.

The largest atomic contributions are the monocentric ones. The adjacent atoms contribute much less to the field gradient; adjacent heteroatoms (O, N) contribute however much more than adjacent C and H atoms (see also Sect. 3.5).

Among the CGTF contributions, the most important ones come from the nitrogen $2p$ type functions. When two CGTF's are used for describing the $2p$ electronic distribution, the largest effect is due to the "internal" CGTF containing the GTF's with highest exponents.

3) *Basis set effects* on the computed field gradients:

Although qualitatively meaningful, but systematically overestimated, coupling constants may be obtained with a wavefunction using a minimal basis set of atomic functions, only an extended basis set may be expected to yield quantitatively significant values.

Not unexpectedly, the computed field gradients are especially sensitive to the p functions on the nitrogen site.

Furthermore the inclusion of d polarization functions on nitrogen may prove also to be of importance.

We thank Drs. H. Basch, J. L. Calais, J. F. Harrison and P. Pyykkö for sending us test calculations for checking our program and Drs. H. Basch and G. Berthier for communicating to us the molecular wavefunctions of some of the nitrogen containing heterocycles.

Note Added in Proof: For recent experimental results on the ^{14}N nuclear quadrupole coupling constants in imidazole III, see: Koo, J., Hsieh, Y.-N.: Chem. Physics Letters **9**, 238 (1971).

References

1. Lucken, E. A. C.: Nuclear quadrupole coupling constants. London-New York: Academic Press 1969.
2. O'Konski, C. T.: In: Determination of organic structures by physical methods, Vol. 2, Chap. 11. New York: Academic Press 1962.
3. Scrocco, E.: Advances chem. Physics **5**, 318 (1963).

4. Townes, C. H., Dailey, B. P.: J. chem. Physics **17**, 782 (1949).
5. Cotton, F. A., Harris, C. B.: Proc. nat. Acad. Sci. USA **56**, 12 (1966).
6. Lucken, E. A. C.: Trans. Faraday Soc. **57**, 729 (1961).
7. Sichel, J. M., Whitehead, M. A.: Theoret. chim. Acta (Berl.) **11**, 263 (1968).
8. Kochanski, E., Lehn, J. M., Lévy, B.: Chem. Physics Letters **4**, 75 (1969).
9. Kern, C. W., Karplus, M.: J. chem. Physics **42**, 1062 (1965).
10. — J. chem. Physics **46**, 4543 (1967).
11. Harrison, J. F.: J. chem. Physics **47**, 2990 (1967).
12. O'Konski, C. T., Ha, T.-K.: J. chem. Physics **49**, 5354 (1968).
13. Bonaccorsi, R., Scrocco, E., Tomasi, J.: J. chem. Physics **50**, 2940 (1969).
14. Ha, T.-K., O'Konski, C. T.: J. chem. Physics **51**, 460 (1969).
15. Pyykkö, P., Calais, J. L.: Research Report N° 160, University of Uppsala, Sweden (1966).
16. Kochanski, E.: Doctorat d'Etat Thesis, Chemistry Department, University of Strasbourg (1969).
17. Clementi, E., Davis, D. R.: J. comput. Physics **2**, 223 (1967); Veillard, A.: IBMOL Version 4, Special IBM technical report, San Jose, California (1968).
18. — Clementi, H., Davis, D. R.: J. chem. Physics **46**, 4725 (1967).
19. Berthier, G., Praud, L., Serre, J.: International Conference on Quantum Aspects of Heterocyclic Compounds in Chemistry and Biochemistry, Jerusalem, March 31–April 5 (1969).
20. Clementi, E.: J. chem. Physics **46**, 4731 (1967).
21. — J. chem. Physics **46**, 4737 (1967).
22. Kochanski, E., Lehn, J. M.: Theoret. chim. Acta (Berl.) **14**, 281 (1969).
23. Lehn, J. M., Munsch, B.: Theoret. chim. Acta (Berl.) **12**, 91 (1968).
24. Veillard, A., Lehn, J. M., Munsch, B.: Theoret. chim. Acta (Berl.) **9**, 275 (1968).
25. Lehn, J. M., Munsch, B., Millié, Ph., Veillard, A.: Theoret. chim. Acta (Berl.) **13**, 313 (1969).
26. — — — Theoret. chim. Acta (Berl.) **16**, 351 (1970).
27. Veillard, A.: Theoret. chim. Acta (Berl.) **5**, 413 (1966).
28. Moireau, M.-Cl., Veillard, A.: Theoret. chim. Acta (Berl.) **11**, 344 (1968).
29. Sternheimer, R., Foley, H. M.: Physic. Rev. **92**, 1460 (1953).
30. Lin, C. C.: Physic. Rev. **119**, 1027 (1960).
31. Nygaard, L., Nielsen, J. T., Kirchheimer, J., Maltesen, G., Rastrup-Andersen, J., Sörensen, G. O.: J. molecular Structure **3**, 491 (1969).
32. Guibé, L., Lucken, E. A. C.: Molecular Physics **14**, 73 (1968); Schempp, E., Bray, D. J.: Physics. Letters **25** A, 414 (1967).
33. Mackrodt, W. C., Wardley, A., Curnuck, P. A., Owen, N. L., Sheridan, J.: Chem. Comm. **1966**, 692.
34. Sörensen, G. O.: J. molecular Spectroscopy **22**, 325 (1967).
35. Guibé, L., Lucken, E. A. C.: Molecular Physics **10**, 273 (1966); Schempp, E., Bray, D. J.: J.chem. Physics **46**, 1186 (1967).
36. Basch, H., Robin, M. B., Kuebler, N. A., Baker, C., Turner, D. W.: J. chem. Physics **51**, 52 (1969); Robin, M. B., Basch, H., Kuebler, N. A., Wiberg, K. B., Ellison, G. B.: J. chem. Physics **51**, 45 (1969).
37. Pierce, L., Dobyns, V.: J. Amer. chem. Soc. **84**, 2651 (1962).
38. Scharpen, L. H., Wollrab, J. E., Ames, D. P., Meritt, J. A.: J. chem. Physics **50**, 2063 (1969).
39. Wollrab, J. E., Scharpen, L. H., Ames, D. P., Merritt, J. A.: J. chem. Physics **49**, 2405 (1968).
40. Weiss, M. T., Strandberg, M. W. P.: Physic. Rev. **83**, 567 (1951).
41. Kemp, M. K., Flygare, W. H.: J. Amer. chem. Soc. **90**, 6267 (1968).
42. Sastry, K. V. L. N., Curl, Jr., R. F.: J. chem. Physics **41**, 77 (1964).
43. Lide, D. R., Jr., Mann, D. E.: J. chem. Physics **27**, 868 (1957).
44. Abe, Y., Kamishina, Y., Kojima, S.: J. physic. Soc. Japan **21**, 2083 (1966).
45. Davies, D. W., Mackrodt, W. C.: Chem. Comm. **1967**, 1226.
46. Love, P.: J. chem. Physics **39**, 3044 (1963); Dehmelt, H. G.: Z. Physik **133**, 528 (1952).
47. Blackman, G. L., Brown, R. D., Burden, F. R.: J. molecular Spectroscopy **36**, 528 (1970).

Professor J. M. Lehn
Institut de Chimie
1 Rue Blaise Pascal
F-67 Strasbourg, France